Ilkogretim Online - Elementary Education Online, Year; Vol 20 (Issue 4): pp. 320-331
http://ilkogretim-online.org
doi: 10.17051/ilkonline.2021.04.34

Analysis of Squeezing characteristics between a Sphere and Rough Porous Flat Plate with variations of Pressure Dependent viscosity by using lubricant additives

Hanumagowda B N, Department of Mathematics, Reva University, Bangalore
Sreekala C K, Department of Mathematics, KNS Institute of Technology Bangalore, sreekalarajeesh@gmail.com
Noor Jahan, Department of Mathematics, Reva University, Bangalore

Abstract- The paper presents an analysis of variation of PDV on the squeeze film lubrication between a sphere and a rough porous plate by using fluids that contain lubricant additives. By using Christensen's stochastic approach, Darcy's formula, Stoke's theory, and Baru's formula modified Reynolds equation is derived which is highly non-linear. The perturbation technique is used to make it linear and expressions for dimensionless pressure, squeezing time and dimensionless load are derived. The predictions are presented graphically.

Key Words: Roughness, pressure dependent viscosity, couple stress fluids, porous

I. INTRODUCTION

The word squeeze has an English origin meaning act of gripping and pressing firmly. The viscosity of the fluid resists the motion and builds fluid pressure to prevent contact between surfaces when they approach each other. Since a limited time is needed to squeeze the viscous liquid out of the gap it has significant effects on bearing characteristics. Nowadays many kinds of research are carried out in the field of squeeze film lubrication mainly with Non-Newtonian couple stress fluids. The simplest broad view of the conventional theory of fluids is Stokes [1] micro continuum theory. Elshaskawy [2] examined the impact of lubricant on the functioning of journal bearings and found that they appreciably boost the load-carrying capability and reduces both frictional coefficient and leakages of sides. Many types of research activities took place like squeeze film performance between the sphere and flat plate [3], partial journal bearings [4], synovial joints [5,6], and stating, an accentuated film pressure, squeezing time, and larger load supporting capacity.

In past years the conditions under which lubricated contacts in machine elements have to operate reliably have become severe. So nominal film thickness has decreased to the level where surface roughness has gained importance. This issue focussed the attention of researchers on the impact of the texture of the surface. Christensen and Tonder [7,8] derived the stochastic Reynolds equation for rough surfaces. Applying Christensen's stochastic theory, the effect of squeeze film lubrication on the roughness of the surface with couple stress fluids as lubricant has been studied by many researchers [9-13].
In earlier studies viscosity μ is treated as a constant. The influence of PDV of the fluid is neglected. But Gould [14] described the changing of viscosity with pressure as significant specifically in squeeze films with high pressure. Recently the authors are more interested in the effects of pressure dependency on viscosity [15-17]. The collective impact of couple stress, PDV and squeeze film lubrication among circular stepped plates was deliberately studied by Hanumagowda [18]. They found that these effects increase fluid film pressure, load carrying capacity, and improve the response time.

Recently Naduvinamani [19] studied the variations of pressure-dependent viscosity on the squeeze film lubrication between a sphere and a rough flat plate with couple stress liquids as a lubricant. The equipment which we are using in everyday life has a porous bearing to support the rotating shaft. They will be supplied with lubricant only once during their manufacture. So the use of porous bearing is a trivial solution as it increases the life of the bearings. The current paper is to analyze the joint effect of PDV, squeeze film lubrication among a rough flat porous plate, and a sphere lubricated with couple stress liquids.

II. MATHEMATICAL FORMULATION

Figure1: ***Configuration of Sphere and Flat Porous plates***

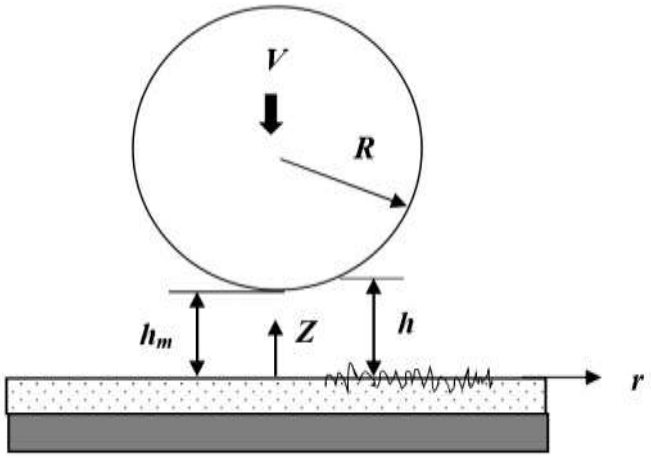

Figure 1 denotes the design under study. Based on the analysis made by Hanumagowda et.al [20] the revised Reynolds equations is

$$\frac{1}{r}\frac{\partial}{\partial r}\left\{\varphi(H,l,\alpha,p)r\frac{\partial p}{\partial r}\right\}=12\mu_0\frac{dH}{dt} \tag{1}$$

where

$$\varphi(H,l,\alpha,p)=e^{-\alpha p}H^3-12l^2He^{-2\alpha p}+24l^3e^{-2.5\alpha p}\tanh\left(e^{0.5\alpha p}H/2l\right)+\frac{12\delta ke^{-\alpha p}}{(1-\beta)} \tag{2}$$

To represent the roughness of a surface, the mathematical equation for film thickness is considered to be consisting of two parts

$$H=h+h_s(r,\theta,\xi) \tag{3}$$

where $h=h_m+\frac{r^2}{2R}$ provided ($r<<R$), denotes the nominal smooth part, while h_s representing the part due to surface roughness asperities.

Taking expectation on either side of equation (1) by Christensen's stochastic theory we have

$$\frac{1}{r}\frac{\partial}{\partial r}\left[E\left\{\varphi(H,l,\alpha,p)\right\}r\frac{\partial E(p)}{\partial r}\right]=12\mu_0\frac{dh}{dt} \tag{4}$$

Normalizing

$$r^*=r/R,\ P^*=-\frac{E(p)h_0^2}{\mu_0R\left(\partial h/\partial t\right)},\ \gamma=-\frac{\mu_0\alpha R\left(\partial h/\partial t\right)}{h_0^2},\ h_m^*=h_m/h_0,\ h^*=h/h_0,$$

$$h_s^*=h_s/h_0,\ H^*=h^*+h_s^*,\ c^*=c/h_0,\ \beta=h_0/R,\ \zeta=l/h_0$$

Substituting these in equation (4) we get

$$\frac{\partial}{\partial r^*}\left[E\left\{\varphi^*(H^*,\zeta,\gamma,p^*)\right\}r^*\frac{\partial P^*}{\partial r^*}\right]=-\frac{12}{\beta}r^* \tag{5}$$

where

$$\varphi^*(H^*,\zeta,\gamma,p^*)=H^{*3}e^{-\gamma p^*}-12\zeta^2H^*e^{-2\gamma p^*}+24\zeta^3e^{-2.5\gamma p^*}\tanh\left(e^{0.5\gamma p^*}H^*/2\zeta\right)+\frac{12\psi e^{\gamma p^*}}{(1-\beta)} \tag{6}$$

Commonly two types of roughness structures are of importance, one-dimensional radial, and azimuthal roughness patterns.

For the one-dimensional radial (azimuthal) roughness pattern, the roughness striations are in the form of long narrow ridges(valleys) running in the radial(*θ)* directions

Hence non- dimensional stochastic film thickness respectively assumes the form

$$H^*=h^*+h_s^*(\theta,\xi) \tag{7}$$

$$H^*=h^*+h_s^*(r,\xi) \tag{8}$$

The modified stochastic Reynold's type equation (5) for these two types of roughness pattern takes the form

$$\frac{\partial}{\partial r^*}\left\{G^*(H^*,\zeta,\gamma,P^*,c^*)r^*\frac{\partial p^*}{\partial r^*}\right\}=-\frac{12}{\beta}r^* \tag{9}$$

where $G^*(H^*,\zeta,\gamma,P^*,c^*)=\begin{cases}E\left\{\varphi^*(H^*,\zeta,\gamma,P^*)\right\} & \text{for radial roughness}\\ \left[E\left\{\dfrac{1}{\varphi^*(H^*,\zeta,\gamma,P^*)}\right\}\right]^{-1} & \text{for azimutal roughness}\end{cases}$

Equation (9) is highly non-linear. The film pressure is expanded for $0\le\gamma<<1$ by substituting

$$P^*=p_0^*+\gamma p_1^* \tag{10}$$

into the equation (9) and perturbating gives the expression for pressure p_0^* *and* p_1^* respectively

$$\frac{\partial}{\partial r^*}\left\{G_0^*(H^*,\zeta,c^*)r^*\frac{\partial p_0^*}{\partial r^*}\right\}=-\frac{12}{\beta}r^* \tag{11}$$

and $$\frac{\partial}{\partial r^*}\left\{G_0^*(H^*,\zeta,c^*)r^*\frac{\partial p_1^*}{\partial r^*}+G_1^*(H^*,\zeta,c^*)p_0^*r^*\frac{\partial p_0^*}{\partial r^*}\right\}=-\frac{12}{\beta}r^* \tag{12}$$

where $G_i^*(H^*,\zeta,c^*)=\begin{cases}E\left[\varphi_i^*(H^*,\zeta)\right] & \text{for radial roughness}\\ \left[E\left\{\dfrac{1}{\varphi_i^*(H^*,\zeta)}\right\}\right]^{-1} & \text{for azimutal roughness}\end{cases}$

for $i=0,1$

$$\varphi_0^*(H^*,\zeta) = H^{*^3} - 12\zeta^2 H^* + 24\zeta^3 \tanh\left(H^*/2\zeta\right) + \frac{12\psi}{(1-\beta)} \text{ and}$$

$$\varphi_1^*(H^*,\zeta) = -H^{*^3} + 6\zeta^2 H^* \left\{4 + \sec^2 h(H^*/2\zeta)\right\} - 60\zeta^3 \tanh\left(H^*/2\zeta\right) - \frac{12\psi}{(1-\beta)^2}$$

Boundary conditions for film pressure are

$$\frac{dP^*}{dr^*} = 0 \text{ when } r^* = 0 \tag{13}$$

$$P^* = 0 \text{ when } r^* = 1 \tag{14}$$

Solving Eqns. (11) and (12) based on boundary conditions (13) and (14) we get

$$p_0^* = \frac{6}{\beta}\int_{r^*}^{1} \frac{r^*}{G_0^*(H^*,\zeta,c^*)} dr^* = \frac{6}{\beta} F_0^* \tag{15}$$

where

$$F_0^* = \int_{r^*}^{1} \frac{r^*}{G_0^*(H^*,\zeta,c^*)} dr^*$$

and

$$p_1^* = -\frac{36}{\beta^2}\int_{r^*}^{1} \frac{G_1^*(H^*,\zeta,c^*)}{\left\{G_0^*(H^*,\zeta,c^*)\right\}^2} F_0^* r^* dr^* \tag{16}$$

By using equations (15) and (16) in (10) gives the dimensionless pressure as

$$P^* = \frac{6}{\beta} F_0^* - \frac{36}{\beta^2}\gamma\int_{r^*}^{1} \frac{G_1^*(H^*,\zeta,c^*)}{\left\{G_0^*(H^*,\zeta,c^*)\right\}^2} F_0^* r^* dr^* \tag{17}$$

Integrating the film pressure to obtain load bearing capacity,

$$E(w) = 2\pi\int_0^R E(p) r dr$$

Dimensionless load bearing capacity is

$$W^* = -\frac{h_0^2 E(w)}{\mu_0 R^3(\partial h/\partial t)} = \frac{12\pi}{\beta^2}\int_0^1 \left[\int_{r^*}^{1} \frac{G_0^*(H^*,\zeta,c^*)\beta r^* - G_1^*(H^*,\zeta,c^*)6\gamma F_0^* r^*}{\left\{G_0^*(H^*,\zeta,c^*)\right\}^2} dr^*\right] r^* dr^* \tag{18}$$

Integrating equation (18) with respect to h_m^* subject to the condition $h_m^* = 1$ at $t^* = 0$

Squeezing Time

$$T^* = \frac{E(w)h_0^2}{\mu R^4} t = \frac{12\pi}{\beta^2}\int_{h_m^*}^{1} \left\langle \int_0^1 \left[\int_{r^*}^{1} \frac{\beta r^* G_0^*(H^*,\zeta,c^*) - 6\gamma F_0^* r^* G_1^*(H^*,\zeta,c^*)}{\left\{G_0^*(H^*,\zeta,c^*)\right\}^2} dr^*\right] r^* dr^* \right\rangle dh_m^* \tag{19}$$

III. RESULTS AND DISCUSSION

3.1Dimensionless film pressure

The deviation of dimensionless pressure P^* against r^* by fixing $h_m^* = 0.8$, is plotted in Figure 2, Figure 3, Figure 4 by respectively varying roughness parameter c^*, pressure dependency parameter γ, and couple stress parameter ζ. In Figure 2 it is noticed that as the values of the roughness parameter (c^*) increase, the azimuthal(radial) pressure increases(decreases). Alsoin Figure 3, Figure 4 it is noticed that as the value of the parameters (γ, ζ) increases pressure increases and azimuthal roughness is more accentuated than radial roughness. In Figure 5 the graph is plotted by varying porosity parameters and by fixing $h_m^* = 0.8$, $\gamma = 0.06$, $c^* = 0.3$, $\zeta = 0.3$ and reverse effect is observed. i.e as the value of porosity (ψ) is increasing the pressure is found to be decreasing.

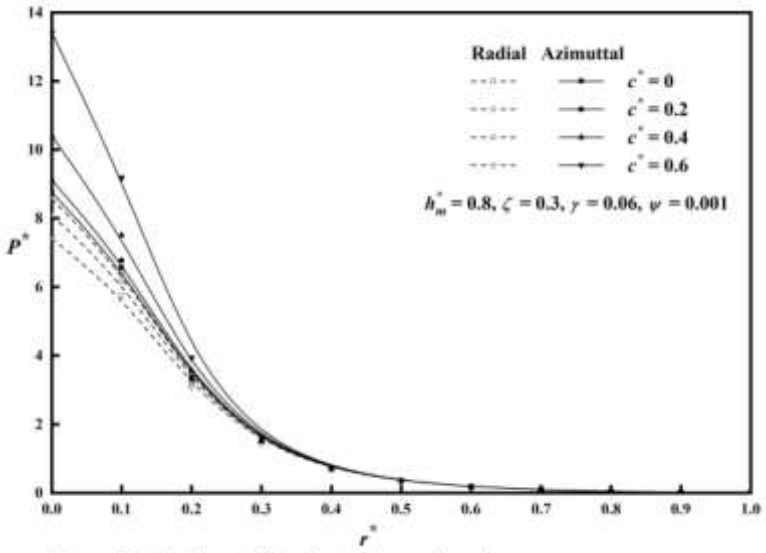

Figure 2: Variation of P^* against r^* by varying c^*

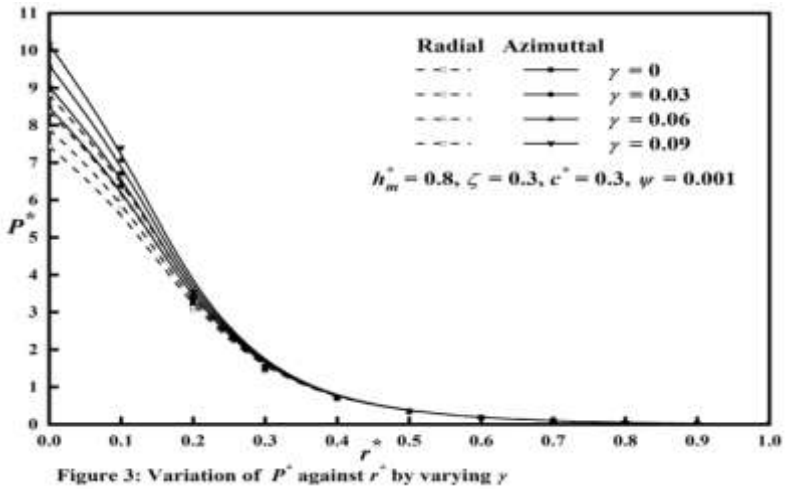

Figure 3: Variation of P^* against r^* by varying γ

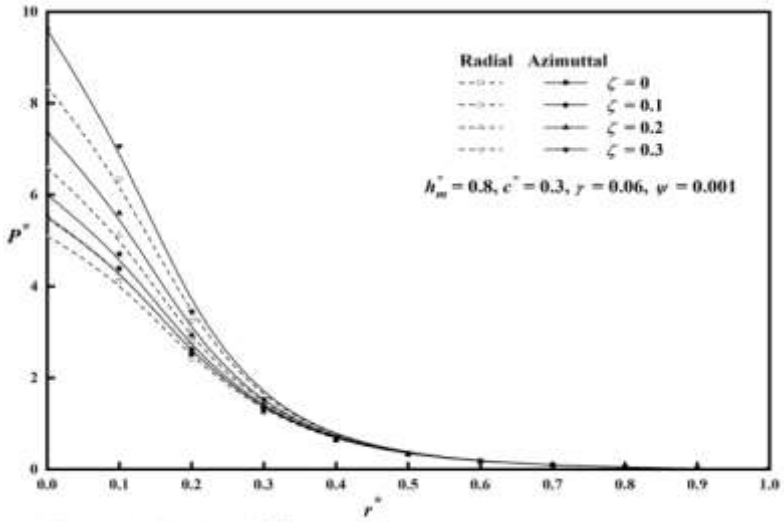

Figure 4: Variation of P^* against r^* by varying ζ

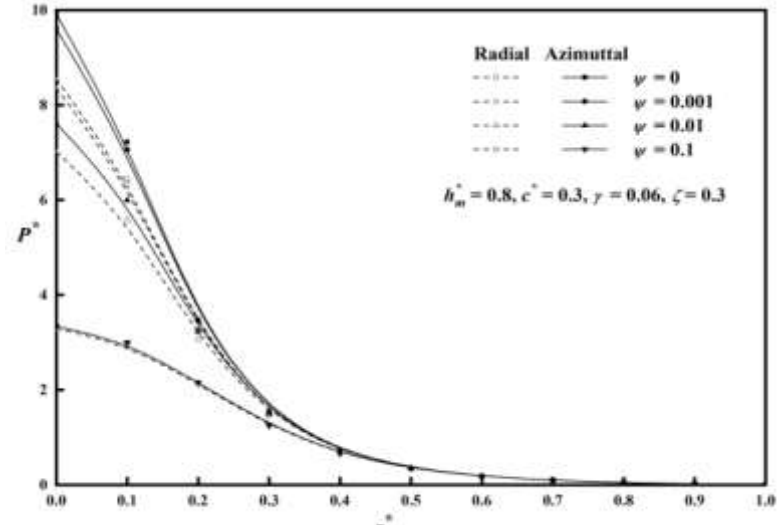

Figure 5: Variation of P^* against r^* by varying ψ

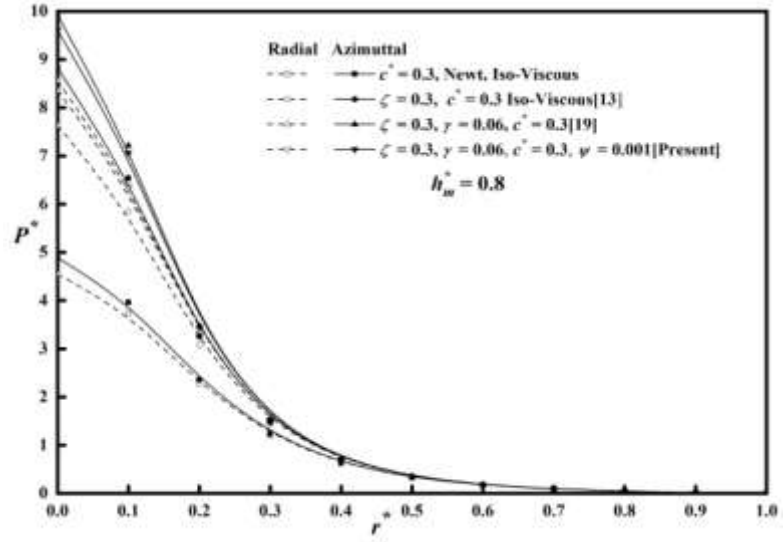

Figure 6: Variation of P^* against r^*

3.2 Dimensionless load carrying capacity

The dimensionless load-bearing capacity is a function of couple stress parameter, pressure-dependent viscosity, roughness, and porous parameters. Figure 7, Figure 8, Figure 9, and Figure 10 represent the changes of dimensionless pressure against h_m^*. In Figure 7 the graph is plotted by varying roughness parameter c^* and is seen that load-bearing capacity increases(decreases) for azimuthal (radial) roughness patterns. In Figure 8, Figure 9 it is seen that dimensionless load-bearing capacity rises with increasing values of couple stress parameter, pressure dependency parameter, and graph indicate that azimuthal roughness pattern has a more prominent load-carrying capacity than radial roughness. In Figure 10 graph is drawn by varying permeability parameter ψ. It is visible that as the value of the porosity parameter rises the load carrying capacity decreases.

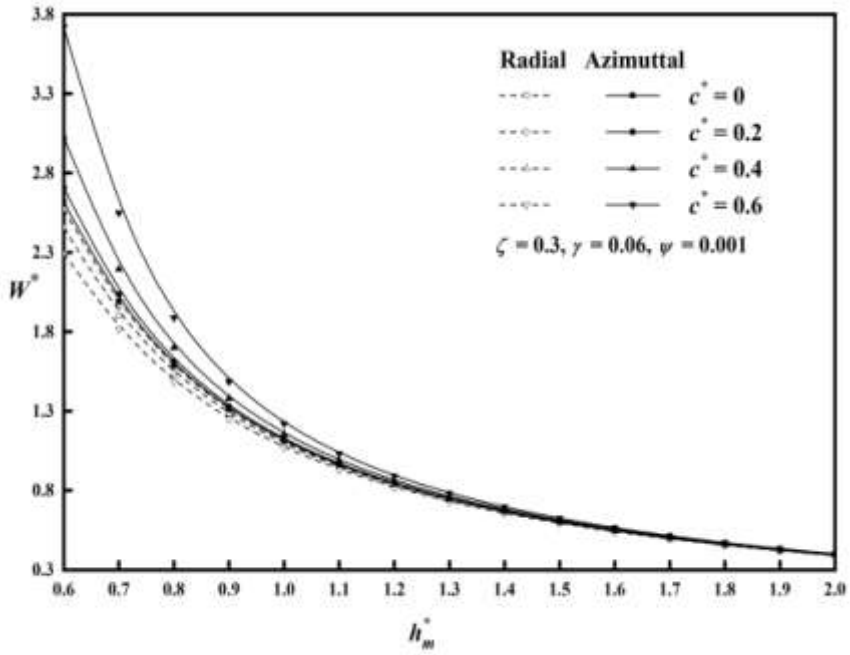

Figure 7: Variation of W^* against h_m^* by varying c^*

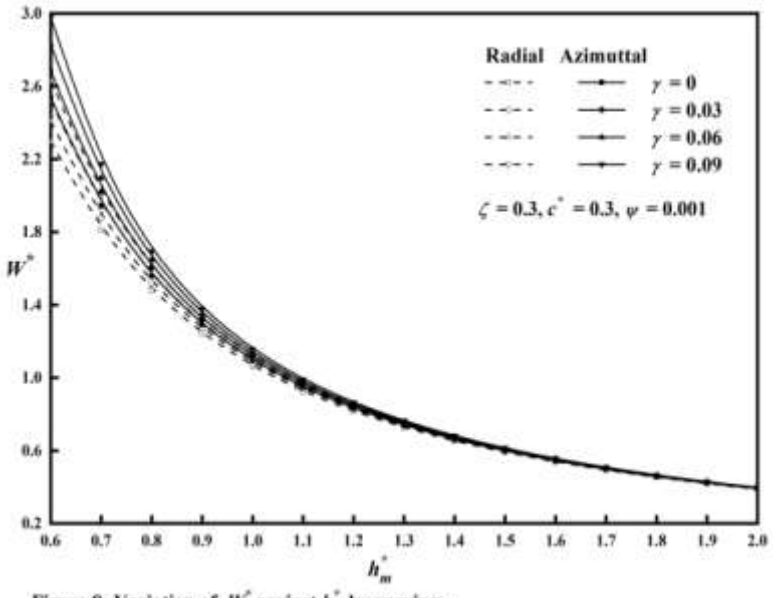

Figure 8: Variation of W^* against h_m^* by varying γ

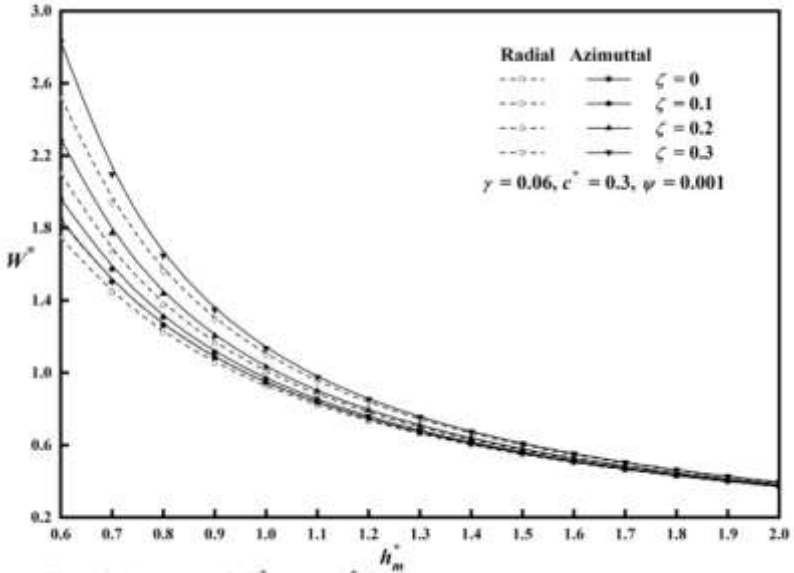

Figure 9: Variation of W^* against h_m^* by varying ζ

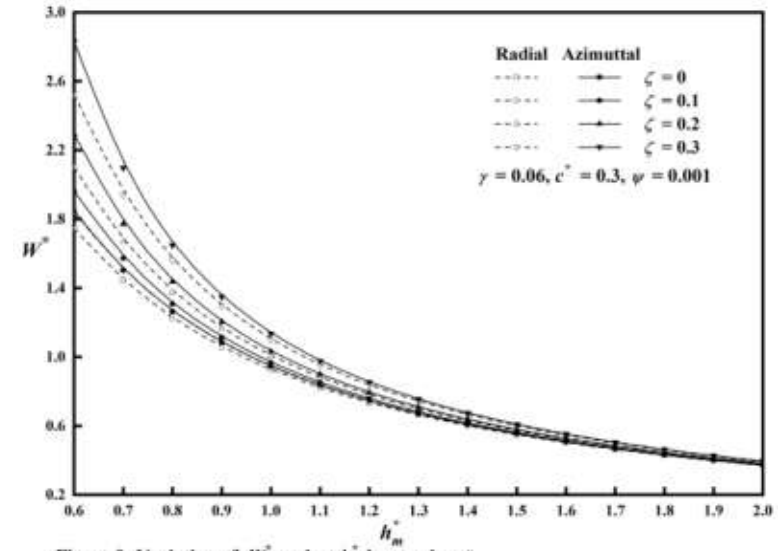

Figure 9: Variation of W^* against h_m^* by varying ζ

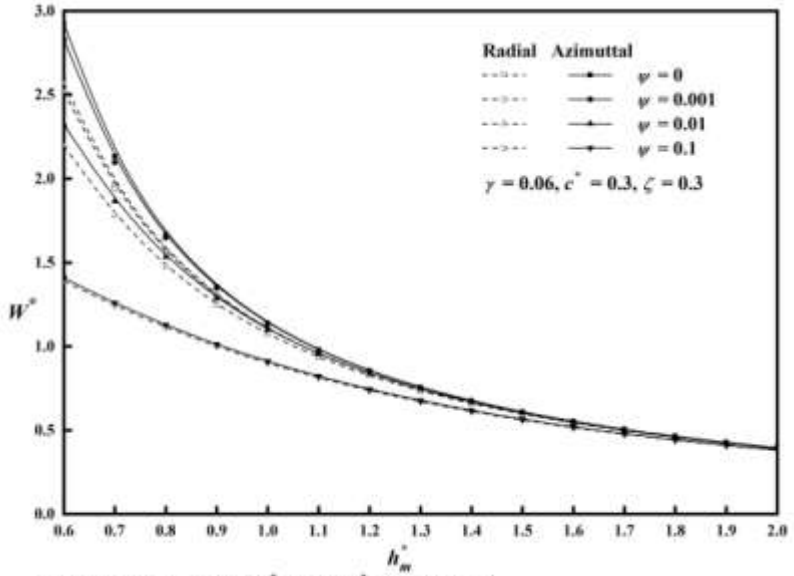

Figure 10: Variation of W^* against h_m^* by varying ψ

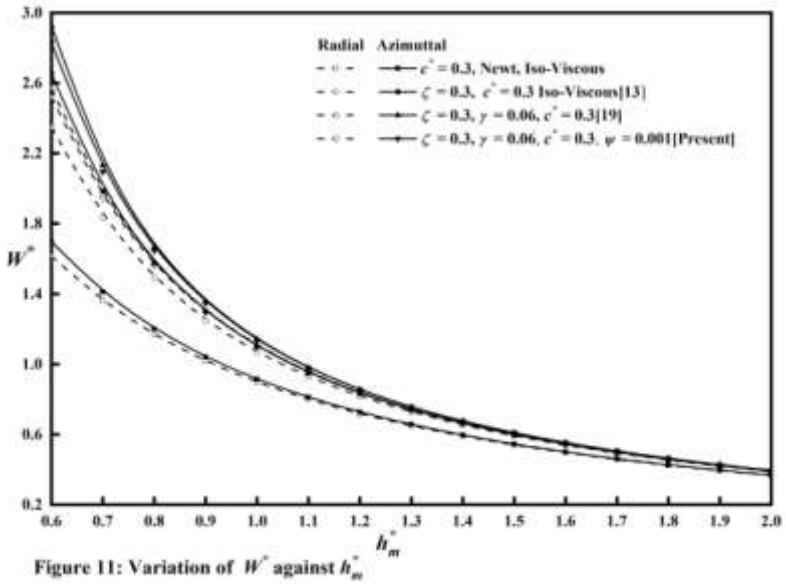

Figure 11: Variation of W^* against h_m^*

3.3 Time-Height Relationship

Figures 12-15 respectively depict the time-height relationship for different values of roughness, pressure dependency, and couple stress parameter by keeping other parameters fixed. In Figure 12, as we increase the value of roughness parameter squeezing time T^* increases for azimuthal roughness whereas an opposite trend is visible for radial roughness and Figure 13 and Figure 14 respectively show that, as we increase the values of pressure dependency parameter and couple stress parameter squeezing time increases. In Figure 15 it is clear that subject to improvement in the value of permeability (ψ)the squeezing time T^* decreases.

Figure 6, Figure11, and Figure16 respectively represent plots of non-dimensional pressure p^*, load bearing capacity W^*, and squeezing time T^* by considering fluids like Newtonian, Non-Newtonian, iso viscous, piezo viscous, and nonpermeable and permeable bearing for a rough surface. The lines are plotted for radial and azimuthal roughness patterns. As ($\gamma \rightarrow 0.0$, $\psi \rightarrow 0.0$) it reduces to Naduvinamni[13] et.al observations whereas $\psi \rightarrow 0.0$ it reduces to Naduvinamnai[19] et. al. analysis.

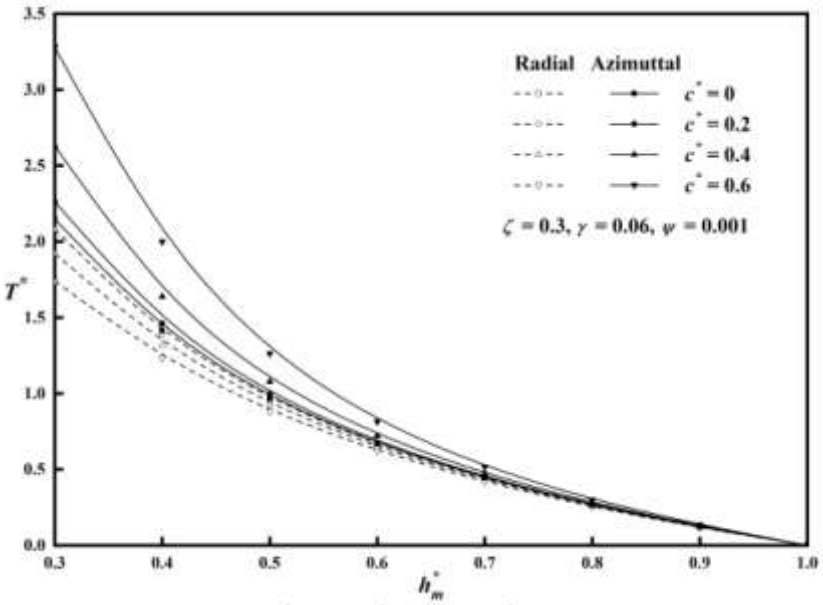

Figure 12: Variation of T^* against h_m^* by varying c^*

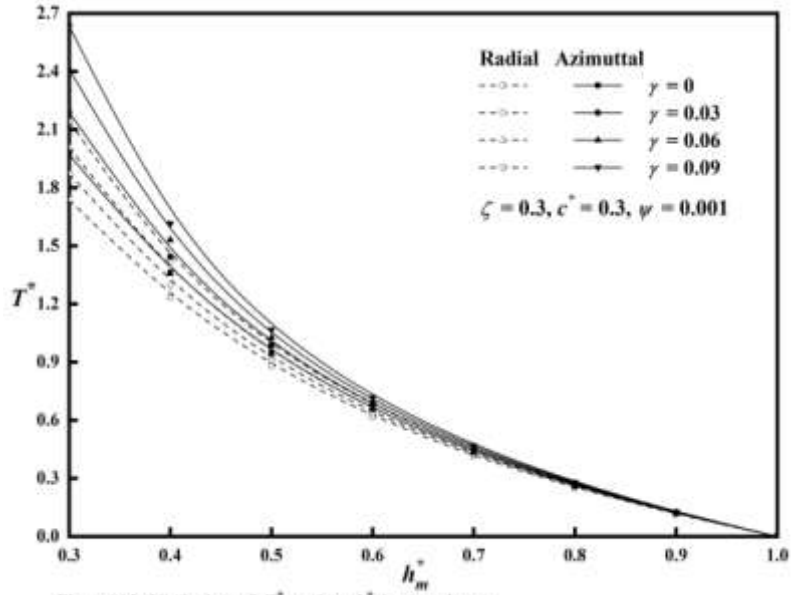

Figure 13: Variation of T^* against h_m^* by varying γ

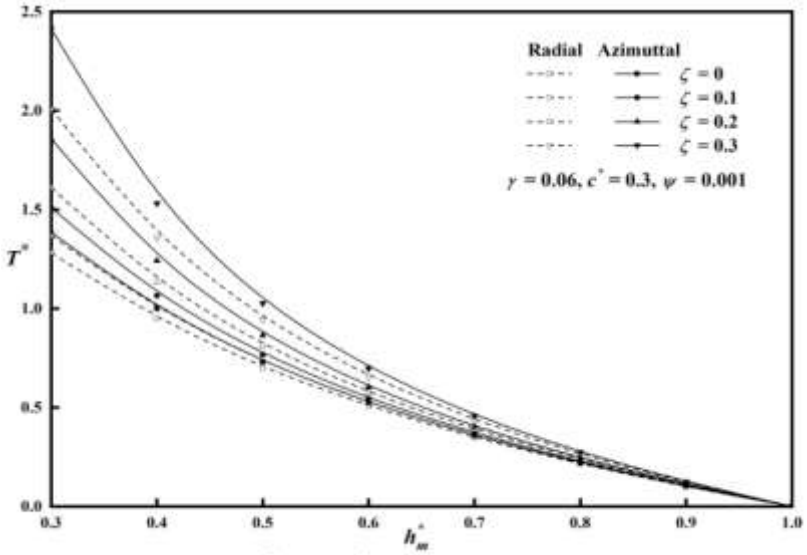

Figure 14: Variation of T^* against h_m^* by varying ζ

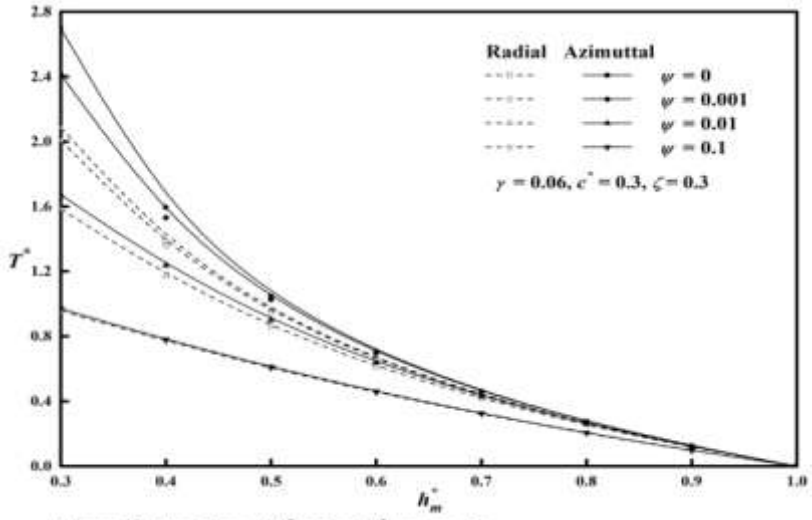

Figure 15: Variation of T^* against h_m^* by varying ψ

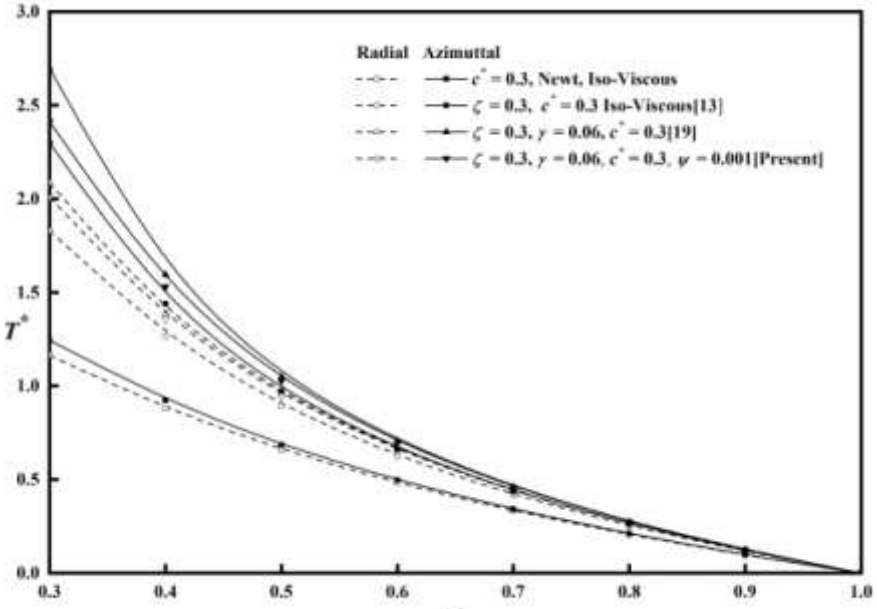

Figure 16: Variation of T^* against h_m^*

IV. CONCLUSION

Based on Baru's expression, Christensen's Stochastic theory, Stokes's theory, and Darcy's equation the impact of PDV on squeeze film lubrication amid a sphere and a rough porous plate lubricated with couple stress fluids are analyzed. Based on it the following conclusions are drawn.

1. As the value of the permeability parameter ψ increases the pressure, load bearing capacity, and squeezing time decreases.
2. Squeeze film characteristics are improved due to the azimuthal roughness pattern on the surface of the bearing whereas the trend is reversed in radial roughness pattern.
3. The pressure, load bearing capacity, and time height relationship is increased when the PDV parameter γ and couple stress parameter ζ increases.
4. When $\gamma \to 0.0$, $\psi \to 0.0$ and $\psi \to 0.0$ this analysis tends to Naduvinamani [13,19] iso-viscous and piezo-viscous nonporous analysis

REFERENCES:

[1] V. K. Stokes. Couple stresses in fluids. J Phys Fluids1966; 9: 1709-1715.
[2] Elsharkawy A.A. Effects of lubricant additives on the performance of hydrodynamically lubricated journal bearing. Tribol Lett 2005; 18: 63–73.
[3] J.R. Lin. Squeeze film characteristics between sphere and a flat plate couple stress fluid model.Computers and Structures 2000; 75: 73-80.
[4] J. R. Lin. Squeeze film characteristics of long partial journal bearings lubricated with couple stress fluids.Tribol International1997; 30: pp. 53-58.
[5] N. M. Bujurke and G. Jayaraman. The influence of couple stresses in squeeze films.*Int J Mech Sci* 1982; 24: 369-376.
[6] J. R. Lin. Couple stress effects on the squeeze film characteristics of hemispherical bearings with reference to synovial joints.*J Appl Mech and Enng*1996; 1: 317-332.
[7] H. Christensen. Stochastic models for hydrodynamic lubrication of rough surfaces. Proceedings of the Institution of Mechanical Engineers1969; 184: 1013–1026.
[8] H. Christensen and K. Tonder. The hydrodynamic lubrications of rough journal bearings. Journal of Lubrication Technology 1973; 95(2):166–172.
[9] J. Prakash and K. Tonder. Roughness effects in circular squeeze plates. ASLE Transactions 1977; 20(3); 257–263.

[10] Vinoth Kumar V, Ramamoorthy S, Dhilip Kumar V, Prabu M, Balajee J.M., "Design and Evaluation of Wi-Fi Offloading Mechanism in Heterogeneous Network", International Journal of e-Collaboration (IJeC), IGI Global, 17(1), 2020..
[11] J. R. Lin, L. C. Hsiu, and C. H. Hsu. Lubrication performance of finite journal bearings considering effects of couple stresses and surface roughness.Tribology International 2004; 37(4):297–307.
[12] J. R. Lin, H. L. Chiang, C. H. Hsu, and Y. P. Chang. Linear stability analysis of a rough short journal bearing lubricated with non-Newtonian fluids.Tribology Letters2004; 17 (4):867–877.
[13] N. B. Naduvinamani, P. S. Hiremath G. and Gurubasavaraja. Effect of surface roughness on the couple-stress squeeze film between a sphere and a flat plate. Tribology International2005; 38: 451–458.
[14] P Gould. High pressure spherical squeeze films. Journal of lubrication technology. 1971; 93(1): 207-208.
[15] C. Barus. Isothermals, isopiestics and isometric relative to viscosity. The American Journal of Science1893; 45: 87–96,
[16] J. R. Lin, L. M. Chu, and W. L. Combined effects of piezo-viscus dependency and non-Newtonian couple stresses in wide parallel-plate squeeze-film characteristics. TribolInt. 2011; 44: 1598–1602.
[17] Umamaheswaran, S., Lakshmanan, R., Vinothkumar, V. et al. New and robust composite micro structure descriptor (CMSD) for CBIR. International Journal of Speech Technology (2019), Vol. 23, Issue 2, pp. 243-249.
[18] B. N. Hanumagowda. Combined effect of pressure-dependent viscosity and couple stress on squeeze film lubrication between circular stepped plates. Proc I Mech E part J, J of Engineering Tribology. 2015; 229(9): 1056-1064.
[19] Karthikeyan, T., Sekaran, K., Ranjith, D., Vinoth kumar, V., Balajee, J.M. (2019) "Personalized Content Extraction and Text Classification Using Effective Web Scraping Techniques", International Journal of Web Portals (IJWP), 11(2), pp.41-52
[20] B. N. Hanumagowda, C.K. Sreekala, Noorjahan, O.D. Makinde. Squeeze Film Lubrication on a Rigid Sphere and a Flat Porous Platewith Piezo-Viscosity and Couple Stress Fluid. Defect and Diffusion Forum. 2020; 401: 140-147.